

Monitoring Human Activity at a Very Local Scale with Ground-Motion Records: The Early Stage of COVID-19 Pandemic in California, U.S.A., New York City, U.S.A., and Mexicali, Mexico

Baoning Wu^{*1}, Roby Douilly¹, Heather A. Ford¹, Gareth Funning¹, Hsin-Yu Lee¹, Shankho Niyogi¹, Manuel Mendoza¹, Christodoulos Kyriakopoulos^{1,2}, and David Oglesby¹

Abstract

In this article, we analyze the change in anthropogenic seismic noise level within a frequency range of 4–14 Hz, through a survey of seismic stations in California, United States, New York City, United States, and Mexicali, Baja California, Mexico from early December 2019 to late April 2020. Our analysis shows that some stations recorded a drop in anthropogenic seismic noise during the COVID-19 pandemic, and the timing of the anthropogenic noise decrease typically correlates with the timing of a strict curtailment of personal and economic activity issued by the local government. In other locations, the drop in the anthropogenic seismic noise appears not to follow the lockdown timing perfectly. During our analysis, we observed that many stations did not record a drop during the early stage of COVID-19 pandemic. Of the 19 stations of the Southern California Seismic Network that were surveyed, we found that only five show a similar extent of drop in anthropogenic seismic noise comparable to the Christmas holiday break in 2019. This suggests that the human activity that caused seismic noise did not significantly reduce during the COVID-19 pandemic near most surveyed stations in southern California. A further analysis implies that the primary seismic noise source in southern California might be traffic, and the continuation of industrial traffic, such as cargo transportation, during the COVID-19 pandemic may be the reason why many stations did not record a noise drop. Our results show that the anthropogenic seismic noise recorded by seismic stations is capable of indicating human activity, and that this metric is, particularly, powerful in measuring how localized communities initially responded to the COVID-19 pandemic.

Cite this article as Wu, B., R. Douilly, H. A. Ford, G. Funning, H.-Y. Lee, S. Niyogi, M. Mendoza, C. Kyriakopoulos, and D. Oglesby (2021). Monitoring Human Activity at a Very Local Scale with Ground-Motion Records: The Early Stage of COVID-19 Pandemic in California, U.S.A., New York City, U.S.A., and Mexicali, Mexico, *Seismol. Res. Lett.* **92**, 3007–3023, doi: [10.1785/0220200257](https://doi.org/10.1785/0220200257).

[Supplemental Material](#)

Introduction

The COVID-19 pandemic caused both tremendous economic hardship as well as reductions in human activity (e.g., [Bonaccorsi et al., 2020](#); [Kraemer et al., 2020](#)). At the time of manuscript preparation (14 November 2020), the total confirmed number of COVID-19 cases has reached 11 million in the United States, with 100,000 more new cases reported each day. This devastating disease first struck the United States in late January 2020, with its first arrival in the states of Washington and California. Soon, it developed into a nationwide pandemic in March, and New York State became the new “hotspot” of COVID-19. To prevent the overloading of hospitals, the state of California and New York took strong mitigation measures to enforce social distancing, hoping to slow the spread of virus, and “flatten the curve” of daily confirmed cases (e.g., [Matrajt and](#)

[Leung, 2020](#); [Thunström et al., 2020](#)). At about the same time, the pandemic also spread in the neighboring country of Mexico. Research has shown that the amplitude of human activity in a city can be correlated with the amplitude of seismic noise near populated areas (e.g., [Gibney, 2020](#); [Lecocq et al., 2020](#); [Poli et al., 2020](#); [Xiao et al., 2020](#); [Guenaga et al., 2021](#)). In the current

1. Department of Earth and Planetary Sciences, University of California, Riverside, Riverside, California, U.S.A., <https://orcid.org/0000-0002-9609-4325> (BW); <https://orcid.org/0000-0003-1724-2535> (RD); <https://orcid.org/0000-0002-8247-0545> (GF); <https://orcid.org/0000-0002-8362-4569> (SN); <https://orcid.org/0000-0002-9022-5056> (MM); <https://orcid.org/0000-0001-9283-2282> (CK); <https://orcid.org/0000-0001-7779-8741> (DO); 2. Center for Earthquake Research and Information, University of Memphis, Memphis, Tennessee, U.S.A.

*Corresponding author: bwu015@ucr.edu

© Seismological Society of America

research, we revisit the early stage of the COVID-19 pandemic in California, United States, New York City, United States, and Mexicali, Baja California, Mexico, with seismic cultural noise recorded by seismic stations.

Human activity has a well-demonstrated ability to generate seismic noise. Such noise can originate from traffic and machinery, and usually has frequency greater than 2–4 Hz (e.g., Stutzmann *et al.*, 2000; McNamara and Buland, 2004; Havskov and Alguacil, 2015). Because anthropogenic, or cultural, seismic noise is rapidly attenuated (on the scale of meters to kilometers from the source) due to its low-amplitude and high-frequency content, a seismometer is typically only sensitive to human activity within a range of a few kilometers (Havskov and Alguacil, 2015). Therefore, seismic data have the potential to provide us with unique information, which we can use to infer how a local community responds to the COVID-19 pandemic.

In this article, we compute the seismic noise amplitude at 4–14 Hz, at several seismic stations in California, United States, New York City, New York, United States, and Mexicali, Baja California, Mexico, from early December 2019 to late April 2020, during which time cases of COVID-19 increased in the United States and Mexico, and strong social-distancing measures were taken by their respective governments. In this study, we show that the seismic noise amplitude at 4–14 Hz reflects the human activity specific to the surrounding local community within a few kilometers' range. At some surveyed stations, a drop in anthropogenic seismic noise is observed concurrently with a social-distancing measure in the area. This is consistent with the high-frequency seismic noise quieting observed at the global scale (Lecocq *et al.*, 2020). However, many stations we surveyed did not record a drop in seismic noise amplitude as had been expected, even though they were near population centers. Our results suggest that the seismic noise amplitude at 4–14 Hz is strongly affected by the human activity at a very local scale (within a few kilometers), and analyzing the patterns in these records may provide unique information on the human behaviors very close to these urban-region stations.

Methods

Measure seismic noise amplitude with displacement root mean square

To measure the seismic noise amplitude within a given time window (from $t = 0$ to $t = T$) at a certain frequency band (from f_1 to f_2), we compute the root mean square (rms) amplitude u_{rms} of the displacement seismogram $u(t)$ from $t = 0$ to $t = T$ at $f_1 - f_2$ frequency band. A comprehensive description of our procedures can be found in Text S1. Here, we will only show a brief summary to illustrate the related concepts. The square of u_{rms} can be defined as follows:

$$u_{\text{rms}}^2 = \frac{1}{T} \int_0^T u^2(t) dt.$$

The rms amplitude u_{rms} at a certain frequency band $f_1 - f_2$ is computed by integrating the power density spectrum $P(\omega)$ of displacement seismogram between $t = 0$ and $t = T$, using Parseval's theorem:

$$u_{\text{rms}}^2 = \int_{f_1}^{f_2} P(\omega) d\omega.$$

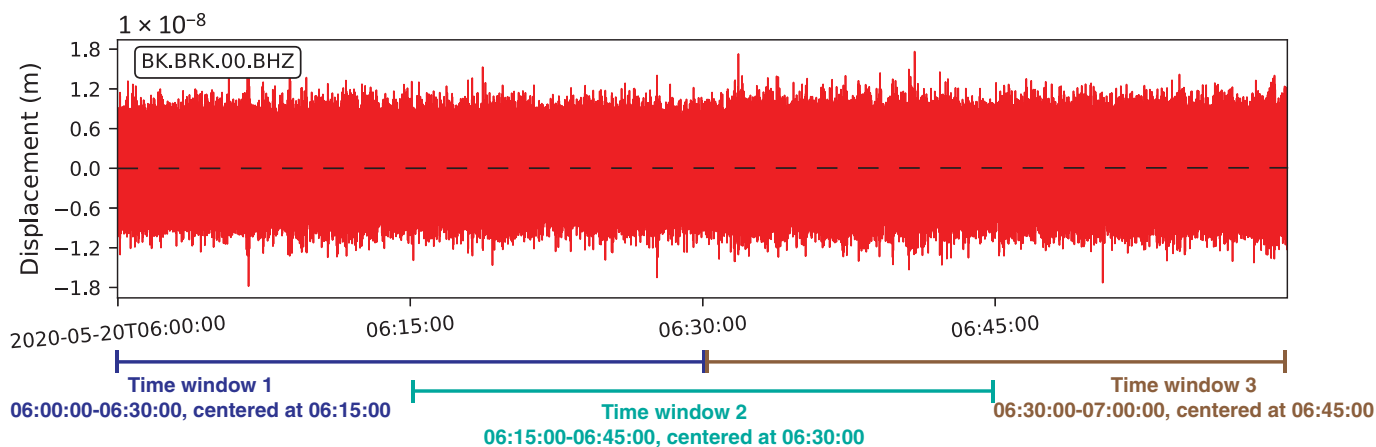
To investigate how the seismic noise amplitude changes with time at a given station, we use a 30 min sliding window (i.e., $T = 30$ min) to scan through its continuous record. Considering that anthropogenic seismic noise is usually found in a frequency range greater than 2–4 Hz (Havskov and Alguacil, 2015), we compute the displacement rms amplitude u_{rms} in a 4–14 Hz frequency band ($f_1 = 4$ Hz, $f_2 = 14$ Hz). The sliding window is offset by 15 min, every time it advances. By scanning the continuous seismic data with the moving time window described earlier, we obtain a displacement rms time series with a sampling interval of 15 min. This time series is capable of showing cultural noise variation within a day.

However, the day-to-day variation of amplitude is not clear in the time series with a sampling rate of 15 min. In addition, short-duration (within a few seconds) tectonic events, such as earthquakes, can occur occasionally in the continuous dataset and make the direct analysis difficult. To compute the daily seismic noise amplitude, we take the median value of the 15 min interval displacement rms time series of a certain day as the seismic noise amplitude of that day. We take the median of displacement rms, rather than the average, to provide a representative value, because the median is less affected by outliers such as seismic events, allowing us to exclude earthquake effects in our analysis without explicitly removing them from our data. In the daily median displacement rms time series, we have a single data point per day (i.e., sampling rate is one day), and we neglect the human activity variation within a day.

Determining the direction of maximum horizontal amplitude ϕ

To discriminate between noise sources, we determine the direction ϕ of the maximum horizontal displacement seismogram amplitude, measured clockwise from north. We use it as a potential indicator for noise source direction. We use the processing procedure developed in Tanimoto *et al.* (2006). Here, we demonstrate only the key concepts; the detailed procedures can be found in Text S2. We use a 30 min sliding window to scan through the continuous record, with an overlap of 15 min. For a given 30 min time series, we first compute the discrete Fourier transform of north and east component displacement seismograms $N(\omega_i)$ and $E(\omega_i)$. Then, we find the direction ϕ that maximizes the following quantity I :

$$I = \sum_{\omega_i=4 \text{ Hz}}^{14 \text{ Hz}} |N(\omega_i) \cos \phi + E(\omega_i) \sin \phi|^2,$$



in which I , as a function of ϕ , repeats every 180° ; therefore, we define $\phi \in [0^\circ, 180^\circ)$. We denote ϕ_m as the direction that yields the maximum I_m . If the seismic noise at 4–14 Hz is primarily Rayleigh waves in horizontal-component seismograms, ϕ_m or $\phi_m + 180^\circ$ would indicate the direction that noise comes from. However, unambiguously proving that the noise in our horizontal-component seismograms at 4–14 Hz is due to Rayleigh waves is nontrivial and is beyond the scope of our article. Therefore, we assume in this study that the seismic noise is predominantly Rayleigh waves and only use ϕ_m as a potential indicator for noise source direction.

Ambient noise cross correlation

We also use ambient noise cross correlation to indicate the noise source direction. As supporting evidence, we calculate the Z component cross correlation of one station pair, CLRSS and AM.R2FCF. Rather than finding the travel-time information in the cross-correlation function, our goal is to find asymmetric pulses in the cross-correlation function, from which we can learn the dominant noise propagation direction between two stations. Our data preparation and cross-correlation procedures follow [Bensen et al. \(2007\)](#) with some modifications. We use the raw vertical seismograms from 1 January 2020 to 15 March 2020 for both stations, cut to multiple time series with length of one day, remove instrument response to displacement, remove mean, remove trend, and band-pass filter at 4–14 Hz. We then apply the “one-bit” normalization to the seismogram, which retains only the sign of the raw signal by replacing all positive amplitudes with 1 and all negative amplitudes with -1 . This procedure reduces the effect of the cross correlations of earthquakes, instrumental irregularities, and nonstationary noise sources near stations. Finally, we compute the cross correlation of each day and stack them. We do not perform the spectral whitening procedure in [Bensen et al. \(2007\)](#).

Results

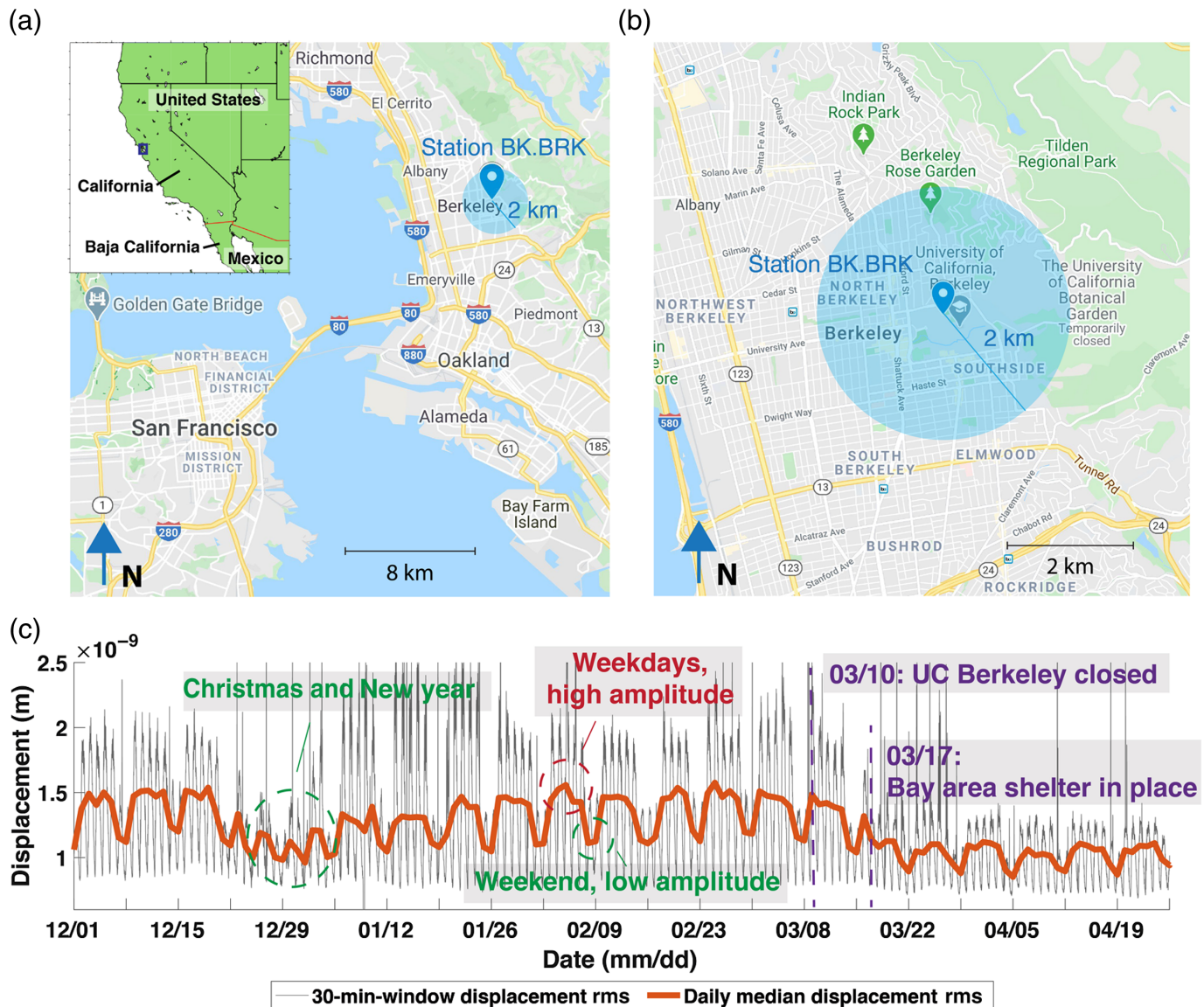
We divide this section into three parts. We first demonstrate an example of station BK.BRK to show the workflow of

Figure 1. An example of a seismic record demonstrating how the sliding time windows are used to compute displacement root mean square (rms) time series. The seismogram in red is 1 hr of a vertical-component seismogram (BHZ) at station BK.BRK filtered at 4–14 Hz (from 20 May 2020, 6 a.m. to 7 a.m., local time). The blue, cyan, and brown horizontal lines below the plot denote the three, 30 min long overlapping sliding time windows within this one hour. The color version of this figure is available only in the electronic edition.

calculating seismic noise amplitude. This station has been investigated by [Lecocq et al. \(2020\)](#), and a lockdown noise reduction is observed. We then analyze the seismic noise amplitude at 4–14 Hz at 23 stations in southern California, United States, to demonstrate the spatial variability of seismic noise drop during the COVID-19 lockdown. Finally, we analyze two more stations outside California within the same period for comparative purposes: LD.CPNU at Central Park in New York City, United States, and BC.UABX at downtown Mexicali, Baja California, Mexico.

Seismic noise drops due to government restrictions: An example from station BK.BRK in Berkeley, California

To demonstrate the workflow, we will show an example with station BK.BRK (Figs. 1 and 2). BK.BRK is a seismic station on the campus of the University of California, Berkeley (Fig. 2a,b), located within the city of Berkeley in the San Francisco Bay Area of California, one of the most densely populated areas in the United States. [Lecocq et al. \(2020\)](#) has observed a lockdown noise reduction at this station. In Figure 1, we show a one-hr seismic record (06:00–07:00) from station BK.BRK. Three windows would be considered for this one-hr record—from 06:00 to 06:30, 06:15 to 06:45, and 06:30 to 07:00. Within each time window, the displacement rms amplitude u_{rms} is computed between 4 and 14 Hz. The results are then used to represent the displacement rms amplitude at the center of each time window, that is, 06:15 for time window 1, 06:30 for time window 2, and 06:45 for time window 3.



We compute the displacement rms of station BK.BRK from 1 December 2019 to 26 April 2020, and the results are shown in Figure 2c. The thin black curves are the displacement rms of the 30 min long sliding window, and the thick red curves show the median displacement rms amplitude for the entire day. Before using the displacement rms to indicate human activity, we need to first confirm that the ground vibration amplitude is primarily anthropogenic. We can confirm this claim by examining three patterns in the displacement rms time series:

1. *Daily pattern:* As shown in Figure 2c, the 15 min interval displacement rms time series shows a strong diurnal periodic pattern. For the month of February 2020, within each 24 hr cycle, the displacement rms has a peak amplitude of about 2 nm during the daytime and a minimum amplitude of about 1 nm during the nighttime.
2. *Weekly pattern:* The daily median of displacement rms shows a strong weekly periodic pattern; it has a peak

Figure 2. (a) Small scale map showing the regional context of station BK.BRK (Berkeley, California). The inset shows the map of California and its neighboring states. The blue rectangle in the inset map denotes the map extent of panel (a). Blue circular shade denotes an area within 2 km of the station. The human activity-induced seismic waves that are detected by the stations are mostly generated within the blue shaded area. (b) Large scale map showing the area near station BK.BRK. (c) Displacement rms of BK.BRK station from 1 December 2019 to 26 April 2020. Thin black curves show the displacement rms of the 30 min-long sliding window, and thick red curves show daily median displacement rms amplitudes. The color version of this figure is available only in the electronic edition.

amplitude of about 1.5 nm during weekdays and a minimum amplitude of about 1.1 nm during weekends. These daily and weekly patterns reflect the prevailing mode of human activity—high in the daytime and weekdays and low in the nighttime and weekends.

3. *Modulation of the weekly pattern in the holidays*: During the Christmas and New Year's holiday in 2019, the ground vibration amplitude dropped about 30%, and the weekly pattern was modulated by the holiday schedule, suggesting a significant decrease in human activity during the public holidays.

Any of the displacement rms patterns above alone might not be compelling enough to support an anthropogenic origin. However, when all three of the patterns coexist, we consider it highly likely that the displacement rms is dominated by anthropogenic noise. In this article, we only use the displacement rms time series for which all three of these patterns indicate the dominance of human activity in the seismic noise. Figure S1, available in the supplemental material to this article, shows the same data as Figure 2c, except that the y axis is extended to include the maximum displacement rms of the 30 min long sliding window. The extreme values shown in Figure S1 are caused by earthquakes that infrequently occur. However, these occasional earthquakes do not affect the daily median displacement rms, and thus will not saturate the low-amplitude anthropogenic noise signal we study.

Once we confirm the dominance of anthropogenic signals in seismic noise, we move forward to investigate the human-activity change around the time when social-distancing restrictions were issued in March 2020 at BK.BRK. As shown in the daily median displacement rms time series in Figure 2c, the weekday daily median displacement rms at station BK.BRK was about 1.5 nm in early December 2019. It dropped to about 1 nm during the Christmas holiday and New Year's holiday. The weekday daily median displacement rms gradually recovered back to its preholiday level in mid-January and stayed at that level until early March.

California was one of the first states in the United States to be affected by the COVID-19 pandemic. The first COVID-19 case was reported by the Center for Disease Control on 26 January 2020 in Orange County (e.g., Linder, 2020; Wigglesworth *et al.*, 2020). As the pandemic intensified in early March, strict restrictions on human activities were ordered by both local and state governments, to stop the spread of the virus (e.g., California Office of the Governor, 2020; Casiano, 2020; Wick, 2020). On 10 March, UC Berkeley suspended most in-person classes (Berkeley News, 2020), and the daily median displacement rms at BK.BRK started to drop (Fig. 2c). At midnight on 17 March, a shelter-in-place order took effect in the Bay Area (Public Health Department, County of Santa Clara, 2020), and the daily median displacement rms at 4–14 Hz underwent a further drop to about 1 nm on weekdays. This level is comparable to that of the 2019 Christmas–New Year holiday. The daily and weekly periodic pattern still persisted afterward, suggesting that cultural noise is still the major contributor of the displacement rms. Human activity is usually not observed in seismic noise beyond a few kilometers from its source (e.g., Havskov and Alguacil, 2015), therefore this result,

at the very best, can only directly constrain human activity in the immediate vicinity of the station BK.BRK. In Figure 2a,b, we use a blue circular shading to denote an area within 2 km of the station. This radius is a first-order empirical estimate of the range of anthropogenic noise sources.

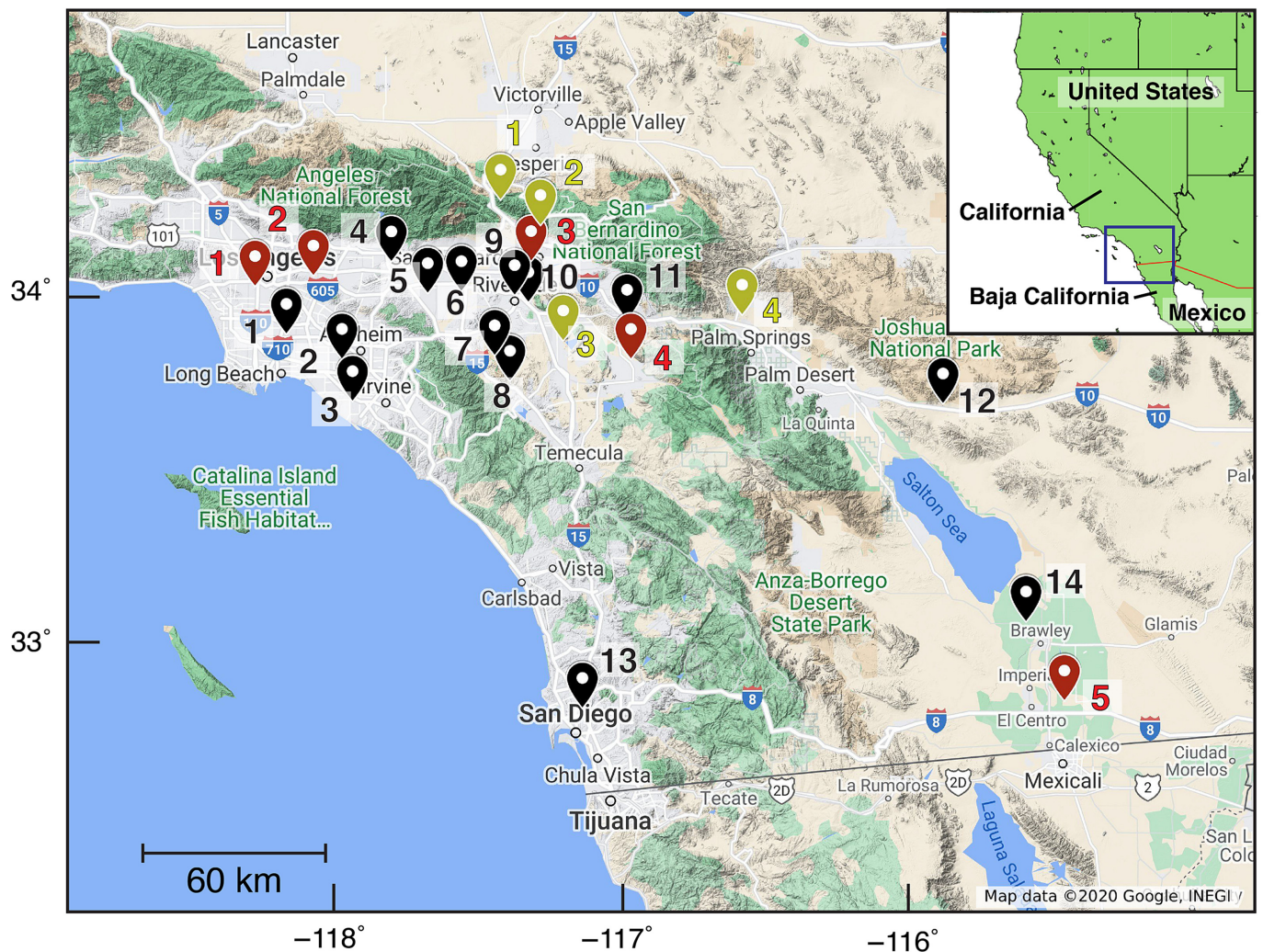
As shown in the case of station BK.BRK, the daily median displacement rms time series shows a clearer daily trend of human activity, compared to the 15 min interval time series. In the remainder of this article, we will only show the daily median displacement rms time series. The 15 min interval time series is not shown, although it was used to check if a diurnal periodic pattern exists.

Spatial variability of seismic noise drops during a shelter-in-place order in southern California

Southern California is one of the most densely populated regions in the United States. It also has one of the densest seismic networks in the world due to the proximity of the San Andreas fault and other dangerous structures in the Pacific-North America plate boundary zone. The Southern California Seismic Network (network code: CI) is the largest seismic network in southern California, operated by the California Institute of Technology (Caltech) and the U.S. Geological Survey in Pasadena (California Institute of Technology and U.S. Geological Survey Pasadena, 1926). Many stations within this network are close to or within significant population centers, and, they provide a valuable dataset to study the human-activity drop patterns in southern California, during the COVID-19 pandemic.

We investigate the displacement rms amplitude at 23 seismic stations in southern California, to obtain an accurate picture of human-activity change in the region. The locations of these analyzed stations are shown in Figure 3. We use the three criteria established in the previous analysis of BK.BRK, to examine whether the seismic noise at a given station is dominated by anthropogenic sources. Out of the 23 stations, 19 of them show a diurnal and weekly cycle and a reduction of signal over Christmas, which are indicative of changes in anthropogenic seismic noise. As will be discussed later, the other four stations do not reflect obvious anthropogenic characteristics (Fig. S4).

To directly compare the 19 time series that reflect human activity, we scale them using the following method: For a given time series, we define the “0” level as the mean of the daily median displacement rms during Christmas–New Year break (21 December 2019–06 January 2020). We define the “1” level as the mean of the daily median displacement rms during a nonholiday period (20 January 2020–29 February 2020). After that, the time series is normalized using the predefined “0” and “1” level. If a time series has amplitude closer to 0 after the shelter-in-place order, it means that the daily median displacement rms amplitude dropped close to the “Christmas” level; conversely, if a time series has amplitude closer to 1, after the stay-at-home order, it means that the daily median displacement rms amplitude remained at the normal nonholiday level.



- 📍 Stations that do not show drop:
 1. CI.LTP 2. CI.BRE 3. CI.LLS
 4. CI.PSR 5. CI.CHN 6. CI.MLS
 7. CI.LMS 8. CI.LMH 9. CI.RVR
 10. CI.RSS 11. CI.BBS 12. CI.CTW
 13. CI.SDG 14. CI.WMD

- 📍 Stations that show drop:
 1. CI.USC 2. CI.RUS 3. CI.CLT
 4. CI.MSJ 5. CI.DRE

- 📍 Stations that show no cultural noise:
 1. CI.CJM 2. CI.IPT 3. CI.PER
 4. CI.DEV

In Figure 4a, we plot all the 19 traces together. The green horizontal dashed line denotes the Christmas–New Year holidays level, and the orange horizontal dashed line denotes the normal nonholiday level. In California, a statewide shelter-in-place order was declared on 19 March 2020 (e.g., Arango and Cowan, 2020; Casiano, 2020; Wick, 2020). As shown in Figure 4a, the patterns of all traces are very similar, before the shelter-in-place order on 19 March. However, the seismic noise amplitude at 4–14 Hz at different stations starts to diverge after 19 March. Fourteen of the 19 stations remained at the normal nonholiday level, whereas, the remaining five stations dropped close to the Christmas level. In Figure 4b, we plot the five stations that show an amplitude drop in red and the other 14 stations that do not show drop in black.

Figure 3. Locations of 23 seismic stations investigated in southern California. The inset shows the map of California and its neighboring states. The blue rectangle in the inset map denotes the map extent of this figure. Red pins denote the five stations that record a drop in human activity after the California shelter-in-place order. Black pins denote the 14 stations that are capable of reflecting human activity variation but did not record a drop in human activity after the California shelter-in-place order. Green pins denote the four stations that appear not capable of reflecting human activity variation. The displacement rms time series of the 19 stations that are capable of reflecting human activity variation are shown in Figure 4. The displacement rms time series of the four stations that do not reflect human activity variation are shown in Figure S4. The color version of this figure is available only in the electronic edition.

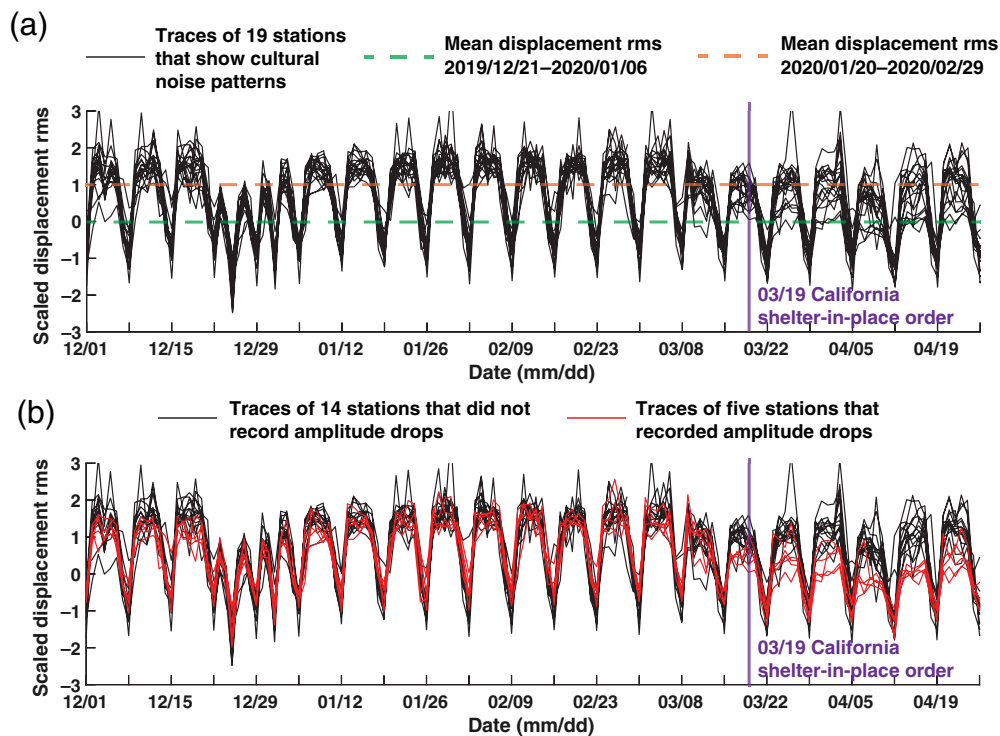


Figure 4. (a) Scaled daily median displacement rms time series of the 19 stations that show the capability of detecting human activity change (black and red pins). All 19 time series are plotted in black. Green horizontal dashed line denotes the Christmas–New Year break level, and Orange horizontal dashed line denotes the normal period level. Vertical purple line denotes the day when California issued a state-wide “shelter-in-place” order. (b) Same as (a), except that the five stations that show an amplitude drop after the shelter-in-place order are instead plotted in red, whereas, the other 14 stations that do not show drop remain plotted in black. The color version of this figure is available only in the electronic edition.

The five stations have very similar trends to the other 14 stations, before the shelter-in-place order in California.

The result above demonstrates a clear spatial variability in anthropogenic seismic noise drop in southern California, after the California shelter-in-place order. The anthropogenic seismic noise level at many locations in southern California surveyed in this study (14 out of 19) did not decrease after the “stay-at-home” order, in contrast to the well-resolved reduction in noise level observed during the Christmas–New Year’s holiday. Because anthropogenic seismic noise mainly originates from traffic and machinery (e.g., Stutzmann *et al.*, 2000; McNamara and Buland, 2004; Havskov and Alguacil, 2015), it might imply that the traffic or industrial activities in southern California did not significantly change after the “stay-at-home” order was enacted. We will further discuss these results in the Discussion section.

Seismic noise changes in Central Park, New York City, and downtown Mexicali, Mexico

The results above suggest that the anthropogenic seismic noise recorded by a seismometer can be used as an indicator of human activity for the nearby community. It is worth noting

that the displacement rms amplitude, at many stations in southern California, did not show a drop concurrent with the timing of California’s stay-at-home order. This result highlights a unique benefit of using seismic noise amplitude to indicate human activity in that it reflects the human activity and societal response to government measures, specific to the surrounding local community, instead of the whole city or state. In this section, we extend our investigation to two other stations outside California, for comparative purposes: station LD.CPNY in Central Park in New York City (another population center in United States) and station BC.UABX on the campus of Autonomous University of Baja California near downtown Mexicali, Baja California, Mexico (a Mexico city bordering southern California). The locations of these two stations are shown in Figure 5a,b.

We compute the displacement rms of stations LD.CPNY and BC.UABX. For reference, we compare them with the displacement rms of station BK.BRK in Berkeley, California, which is discussed previously. Figure 5c plots the daily median displacement rms from 1 December to 26 April of these three stations. In the panel for each station, blue curves show the trend of the pandemic-affected year (December 2019 to April 2020), and gray curves show the trend of the previous year (December 2018 to April 2019), as a comparison. Vertical lines of different colors (numbered in a chronological order) denote the dates when potential human-activity-related measurements were issued, such as a “school closure” order or a “shelter-in-place” order.

As shown in Figure 5c, all three stations show a weekdays–weekend variation pattern in displacement rms records. At station BC.UABX, a decrease in amplitude is concurrent with the Christmas (25 December) and New Year holiday (1 January) for both years. At LP-CPNY, a decrease in amplitude during this same period is not observed, although, the weekday–weekend periodicity does appear to be modulated, suggesting rapidly fluctuating changes in human activity. These results indicate that the seismic noise at these three stations

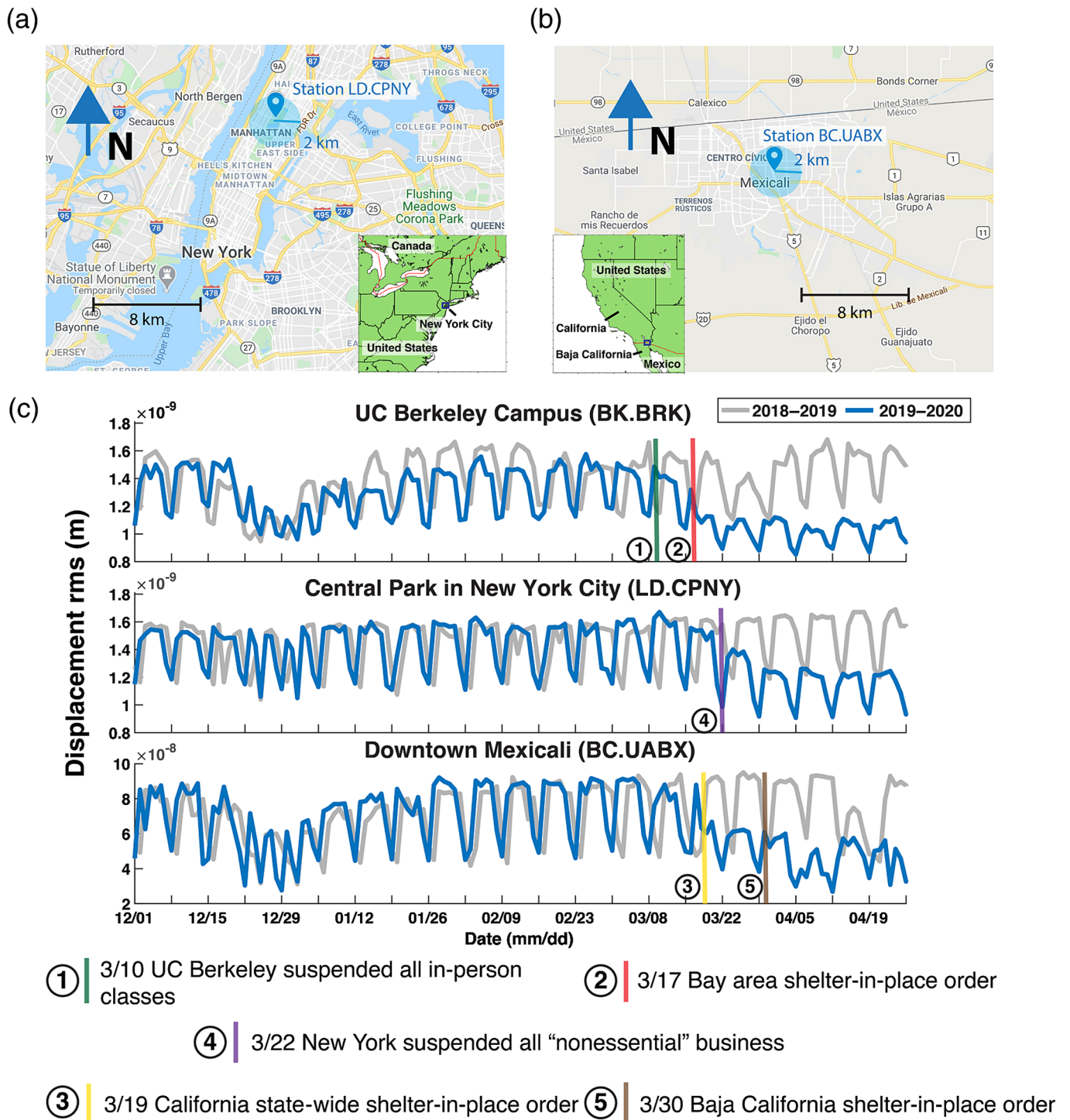


Figure 5. (a) Map showing the area near station LD.CPNY (Central Park, New York City, New York). The inset shows the map of the Northeast region in United States. The blue rectangle in the inset map denotes the map extent of panel (a). Blue circular shade denotes an area within 2 km range of the station. The human activity-induced seismic waves that are detected by the stations are mostly generated with the shaded area. (b) Map showing the area near station BC.UABX (downtown Mexicali, Baja California, Mexico). The inset shows the map of California and its neighboring states. The blue rectangle in the inset map denotes the map extent of

panel (b). Blue circular shaded area is defined as above. (c) Daily median displacement rms time series of BK.BRK (upper panel), LD.CPNY (middle panel), and BC.UABX (lower panel) from 1 December to 26 April. In each panel, blue curves show the trends from December 2019 to April 2020, and gray curves show the trends from December 2018 to April 2019 for comparison. Vertical lines of different colors (numbered in a chronological order) denote the dates when a potential human-activity-related restriction was issued, such as “school close order” or “shelter-in-place order.” The color version of this figure is available only in the electronic edition.

is subject to nearby human activity and, therefore, are capable of reflecting human-activity change. A more speculative reading of our results suggests that individual locations may respond to specific events differently, resulting in differences in the seismic noise record. As an example, we see that amplitude of seismic noise near Central Park (LD.CPNU) does not drop off near the Christmas holidays, in contrast to stations BC.UABX and BK.BRK. This might be due to the fact that human activity near the park did not decrease during holidays.

We then further investigate the displacement rms amplitude before and after the COVID-19 pandemic. Before March 2020, the displacement rms amplitudes at these three stations are very similar to the same period in the previous year. As the COVID-19 pandemic intensified in March 2020, displacement rms began to drop to a level lower than in the previous year (the year 2019). Station BK.BRK on the UC Berkeley campus records a drop in displacement rms amplitude, starting from 10 March, when UC Berkeley was closed, and continued to drop when the shelter-in-place order was issued in the Bay Area on 17 March. At Central Park in New York City, station LD.CPNU records a slight drop of displacement rms amplitude a few days before Governor Andrew Cuomo signed the “New York State on PAUSE” executive order on 20 March, closing 100% of nonessential businesses statewide (New York Office of the Governor, 2020). Displacement rms decreased further when the order took effect on 22 March. One week later, on, approximately, 27 March, the displacement rms amplitude of LD.CPNU dropped to its lowest level.

In the border town of Mexicali, station BC.UABX records a drop in displacement rms amplitude on 17 March. This drop occurred almost concurrently with the state-wide shelter-in-place order in California issued on 19 March. On 30 March, a shelter-in-place order was also issued in Baja California (the Mexican state where Mexicali is located) (e.g., Fry, 2020; Lewis, 2020), almost two weeks after the recorded displacement rms amplitude dropped in Mexicali. This result shows that the change in the anthropogenic noise in downtown Mexicali is correlated with the shelter-in-place order in California, rather than the shelter-in-place order in Baja California. It suggests that human activity in Mexicali is probably strongly influenced by the bordering US state of California.

In summary, we find that, although, the two stations LD.CPNU and BC.UABX recorded a drop in seismic noise in March 2020, the drops did not perfectly coincide with the regional shelter-in-place order. The differences between the state orders and the displacement rms time series suggest that the independent measures of human activity are sensitive to different but complementary aspects of the pandemic response. The anthropogenic seismic noise should reflect the human-activity level in the local area (within several kilometers). We will further discuss this point in the Discussion section.

Discussion

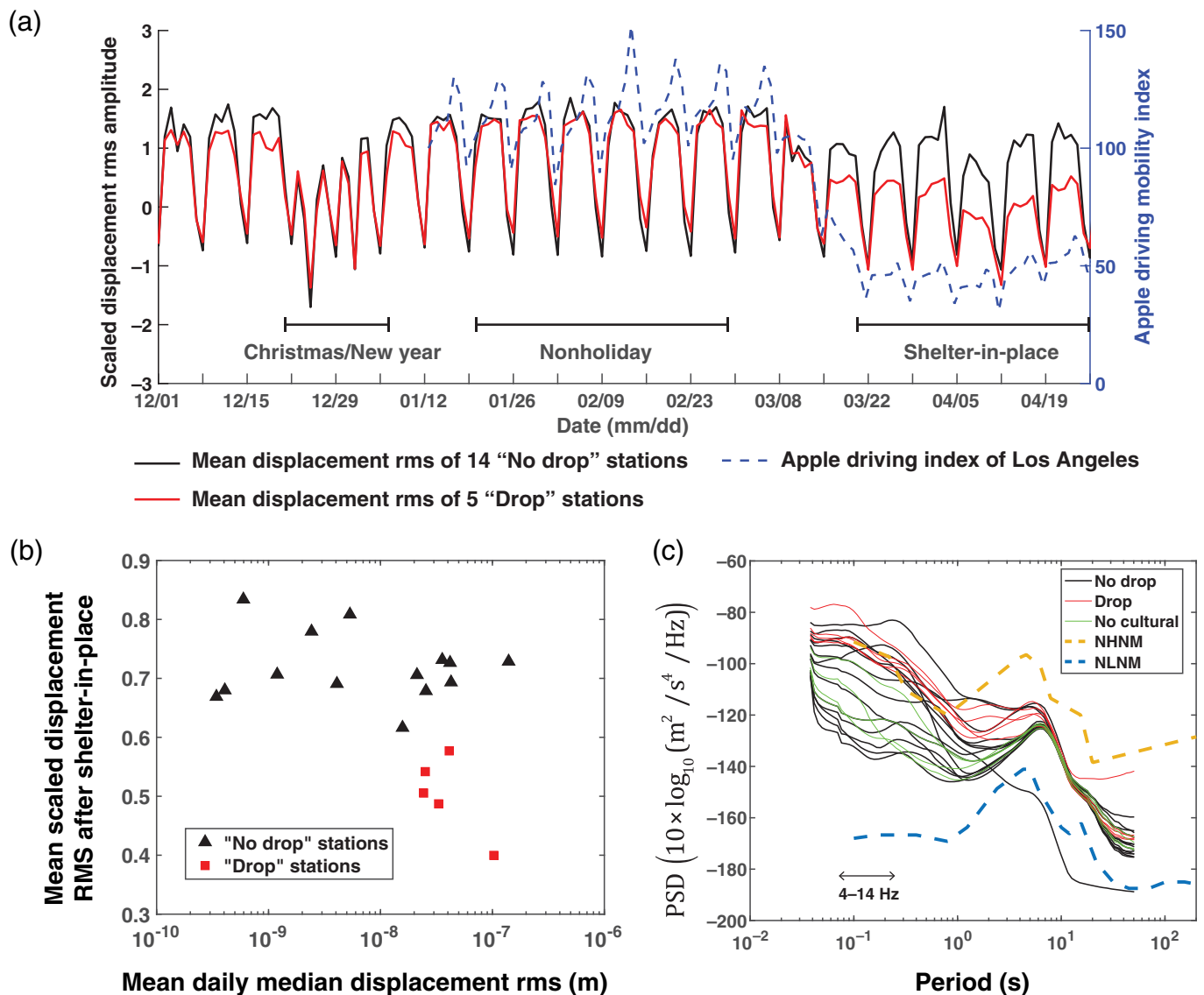
Spatial variability of seismic noise trends in southern California

An interesting observation in our study is that the anthropogenic seismic noise trends in southern California are spatially diverse after the “shelter-in-place” order was implemented. Anthropogenic noise dominates 19 out of the 23 stations we surveyed. As shown in Figure 4, all these 19 stations show very similar trends in displacement rms time series, before the “shelter-in-place” order; after that, five stations recorded a drop in displacement rms amplitude, whereas, the other 14 did not. Figure 6a shows the comparison between the mean displacement rms time series of the five “drop” stations (red solid curve) and the mean displacement rms time series of the 14 “no drop” stations (black solid curve). We can see that the diverse modes in trends start from mid-March (around 15 March). After that, the displacement rms amplitude of the five “drop” stations decreases to near the Christmas–New Year break level; whereas, the displacement rms amplitude of the 14 “no drop” stations still remains close to the nonholiday level. However, a slight decrease is still visible within those 14 stations.

To further investigate this observation, we define the shelter-in-place anthropogenic noise level as the mean value of displacement rms time series between 20 March 2020 and 26 April 2020. In Figure 6b, we plot the scaled shelter-in-place noise level against the absolute nonholiday noise level for all 19 stations that are dominated by anthropogenic noise. All the five stations that we visually identify as having a noise drop after the COVID-19 shelter-in-place order have a scaled shelter-in-place noise level lower than 0.6, whereas, for the other 14 stations the shelter-in-place noise level is higher than 0.6. It is worth noting that stations that recorded a noise drop during shelter-in-place tend to have a higher absolute noise level during the nonholiday period, compared to seven stations that did not record a noise drop. However, there are also seven stations that have a high-absolute noise level during the nonholiday period that did not record a noise drop as well. This result implies that having a high-absolute noise level is necessary but not a sufficient condition for a station to record a noise drop in the shelter-in-place period. This point is further illustrated, when we compare the seismic noise probability density function (PDF) among these 23 stations we survey in southern California (method in Text S3). Figure 6c shows the average power of the PDFs of these stations. All the five “drop” stations have a relatively high-noise level at 4–14 Hz; however, there are also seven “no drop” stations that have a similar high-noise level as well.

Stations that are insensitive to anthropogenic noise sources

In southern California, we found four stations that did not show anthropogenic noise characteristics (CI.CJM, CI.DEV,



CL.IPT, and CL.PER). Their displacement rms time series are shown in Figure S4. Although, all these four stations show some extent of anthropogenic noise characteristics from time to time (diurnal and weekly periodic pattern), their patterns are not stable; so, we do not include them into our analysis.

A comprehensive discussion of why these stations are insensitive to anthropogenic noise sources is beyond the scope of this article. Instead, we pose some hypotheses only based on the data we obtain in this study. As for stations CL.CJM, CL.DEV, and CL.IPT, they are located relatively far from a population center or a dense road network (Fig. 3), so the anthropogenic noise they receive is relatively low (Fig. 6c). In addition, stations CL.CJM, CL.DEV, and CL.IPT are relatively close to the San Andreas fault (within a few kilometers), and the earthquakes nearby may greatly contribute to seismic noise at 4–14 Hz and swamp the anthropogenic noise (Fig. S4a,c). As for station CL.PER, it is neither far away from a population center nor very close to an active fault. However, the baseline of its seismic noise

Figure 6. (a) The red solid line denotes the mean of the five scaled daily median displacement rms time series that record a drop after the shelter-in-place order. The black solid line denotes the mean of the 14 scaled daily median displacement rms time series that did not record a drop after the shelter-in-place order. The blue dashed line denotes the Apple mobility “driving index” of Los Angeles City. (b) The scaled shelter-in-place noise level against the absolute nonholiday noise level for the 19 stations that show anthropogenic noise characteristics. (c) The average power of the seismic noise probability density function (PDF) of the 23 surveyed stations. Red lines are the five stations that record a drop in anthropogenic noise after shelter-in-place order. Black lines are the 14 stations that did not record a drop in anthropogenic noise after shelter-in-place order. Green lines are the four stations that did not show anthropogenic noise characteristics. Yellow and blue dashed lines denote the new high noise model (NHNM) and the new low noise model (NLNM) in Peterson (1993), respectively. The color version of this figure is available only in the electronic edition.

level at 4–14 Hz seems to have a very long period oscillation (Fig. S4d). On top of this long-period oscillation, diurnal and weekly periodic patterns can still be occasionally seen. We are not clear why this long period oscillation exists.

Nevertheless, we note that our hypotheses here are very preliminary and speculative. A thorough study on these null stations is needed in the future, before their behavior can be fully explained.

Traffic as the origin of anthropogenic noise source in southern California

Considering that anthropogenic seismic noise at 4–14 Hz are usually not detected beyond a few kilometers, the 19 stations that show anthropogenic noise characteristics are likely to have noise sources that are different from each other. On the other hand, because the displacement rms of those 19 stations have an almost identical pattern before the shelter-in-place order (Fig. 4), it suggests that the human activities that generate 4–14 Hz anthropogenic noise in southern California might share very similar characteristics at different locations and might be stable through time. Therefore, the variation we see in a station might not come from a noise source that is unique to the locality, such as a generator or air conditioner very close to the station, or a noise source that is transient, such as a nearby construction site in operation for only a short period of time.

A plausible explanation we favor for the noise source is traffic. In southern California, traffic is relatively homogeneous throughout the region. If traffic were the major anthropogenic noise source, it would cause similar noise level trends at different stations far apart. In addition, traffic conditions in southern California are stable through time and, therefore, the weekly pattern in its seismic noise should be stable through time as well. These characteristics are consistent with the displacement rms trends we observe in southern California, making traffic an attractive candidate explanation.

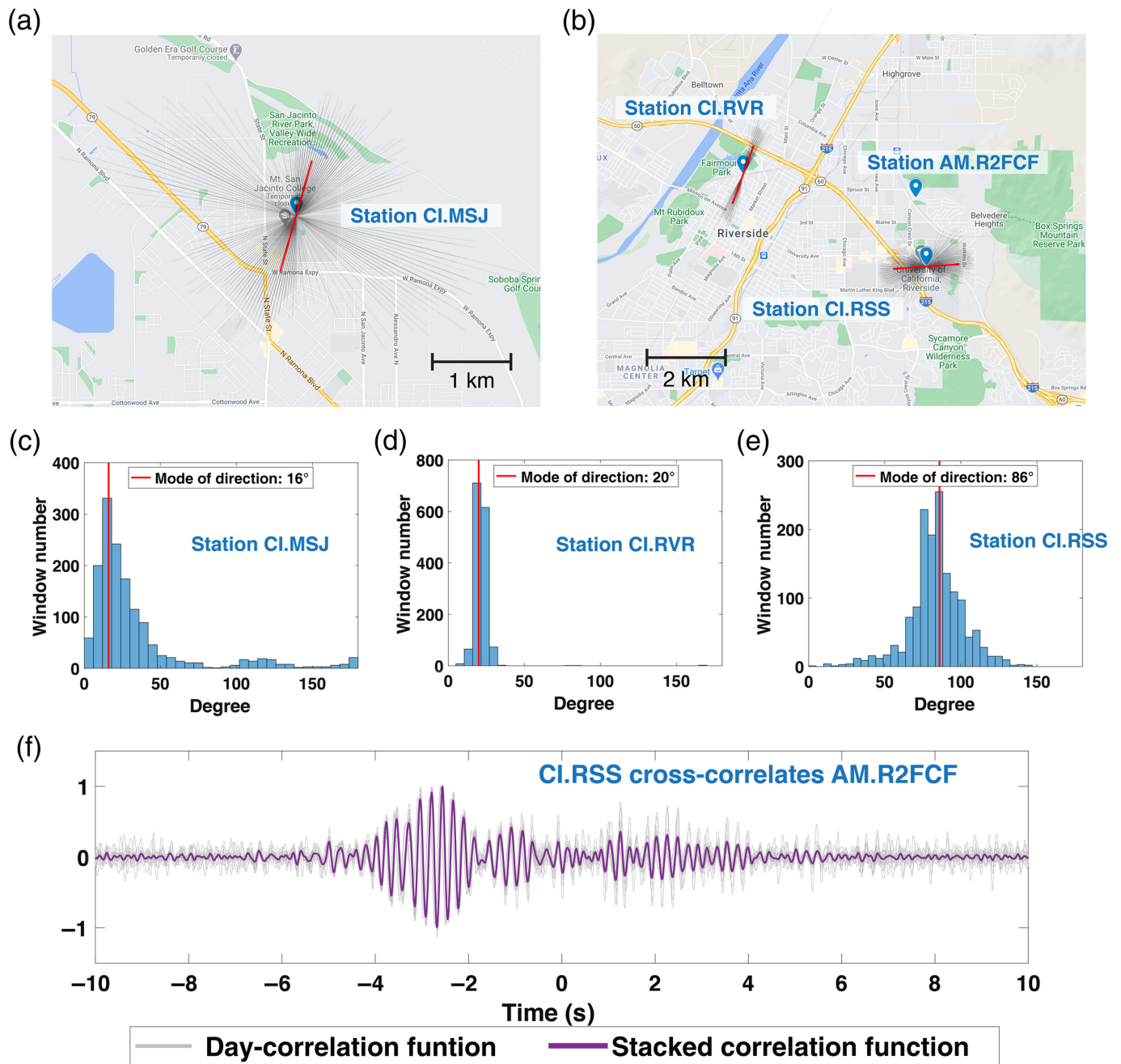
A comprehensive investigation to confirm the noise source could be nontrivial. Because noise above 4 Hz usually cannot be recorded beyond a few kilometers from the source, the local human-activity condition around a station must be well characterized, to make a detailed analysis. A systematic detailed analysis of the noise sources at all the stations we survey will be a subject for a future study. In this part of discussion, we will pick three of our surveyed stations to analyze as an example: CI.MSJ, CI.RVR, and CI.RSS. All these three stations are capable of reflecting human activity; yet, CI.MSJ recorded a drop in human activity after the shelter-in-place order, whereas, CI.RSS and CI.RVR did not. Because these three stations are within the Riverside area, where all the authors of this article are based, we feel relatively comfortable to speak about the human activity in the region both before and after the pandemic.

To investigate the noise source at the different stations, we determine the direction of maximum horizontal amplitude

ϕ_m (with respect to north) of the three stations between 10 and 24 February 2020, a two-week nonholiday period before the shelter-in-place order. Figure 7a,b shows the direction ϕ_m on map. The orientation of a line centered at a station denotes the direction ϕ_m , and the length of line represents the normalized amplitude I_m . Gray thin lines show the ϕ_m of 1469 segments within this period, and the red thick line shows the mode of direction ϕ_m . Figure 7c–e shows the histogram of direction ϕ_m of these three stations, with the red line denoting the mode of direction ϕ_m .

If we assume that the horizontal polarities in our results are mainly caused by Rayleigh waves, the direction ϕ_m or $\phi_m + 180^\circ$ could indicate the direction where noise is coming from. If this assumption were true, our results would strongly suggest that the anthropogenic noise is coming from traffic in the three stations we investigate. For station CI.MSJ, the mode of direction ϕ_m is 16° . It is perpendicular to the California State Route 79, and the direction $\phi_m + 180^\circ = 196^\circ$ is, approximately, pointing to the junction where the California State Route 79 intersects two other major local roads. The histogram of CI.MSJ implies that ϕ_m occasionally changes to about 120° , and the direction $\phi_m + 180^\circ$ is 300° . This direction is perpendicular to a very close major local road that runs north–south. At stations CI.RVR and CI.RSS, the modes of direction are 20° and 86° . These two directions are perpendicular to the nearby California State Route 60, where the traffic is the busiest and the most crowded near the Riverside area. Noticeably, direction ϕ_m rotates as the California State Route 60 makes a slight turn from east to west, and the rotation angle is similar to the road turning angle. This pattern again supports that the anthropogenic noise at 4–14 Hz, at these two stations, originated from traffic.

The above single-station analysis indicates that traffic is the major source of 4–14 Hz seismic noise at these stations, yet, it relies on the assumption that the noise is Rayleigh wave. Ambient noise cross correlation is another helpful tool to investigate the noise source direction; yet, the frequency band we study is so high that even for a close station pair of CI.RSS and CI.RVR that are 5 km apart, their ambient noise did not correlate (Fig. S2). Fortunately, there is a Raspberry Shake station AM.R2FCF that is only 1.6 km away from the station CI.RSS (Fig. 7b). Although, it only has a vertical component, and the accuracy is not as good as a permanent station, this station makes an ambient noise cross-correlation investigation at 4–14 Hz possible. Figure 7f shows the cross-correlation function between CI.RSS.BHZ and AM.R2FCF.EHZ. The gray lines denote the day-correlation function of each 14 day, and the purple line denotes the stack correlation function. There are wave packets of large amplitude on the negative time axis, at around -2.8 s, whereas, there are not such packets on the positive time axis. This result suggests that the dominant correlated noise at these two stations mainly propagates from CI.RSS to AM.R2FCF. This is consistent with our hypothesis that the noise at CI.RSS comes from the California State Route



60. A lag time of 2.8 s of these wave packets and a station separation of 1.6 km imply an average group velocity of 0.57 km/s, suggesting that these wave packets might be the fundamental Rayleigh waves.

The last piece of evidence that supports the traffic hypothesis comes from the comparison with precipitation data. In Figure 8, we compare the average displacement rms with the average daily precipitation in southern California, during the same period (the method to compute the average daily precipitation of southern California can be found in the Text S5). All of the seismic stations sensitive to human activity, whether their displacement rms dropped during the COVID-19 lockdown or not, show a drop during the second week in April

Figure 7. (a,b) Location of CI.MSJ, CI.RVR, CI.RSS, and AM.R2FCF on Google map. The orientation of a gray and red lines centered at a station denotes the direction ϕ_m , and the length of line represents the normalized amplitude I_m . Gray thin lines show the ϕ_m of 1469 segments within the study period, and the red thick line shows the mode of direction ϕ_m . (c–e) Histogram of direction ϕ_m of stations CI.MSJ, CI.RVR, and CI.RSS, respectively. (f) The cross-correlation function between CI.RSS and AM.R2FCF. The gray lines denote the day-correlation function of each 14 day, and the purple line denotes the stack correlation function. Pulse on the negative time axis means signal propagating from CI.RSS to AM.R2FCF. The color version of this figure is available only in the electronic edition.

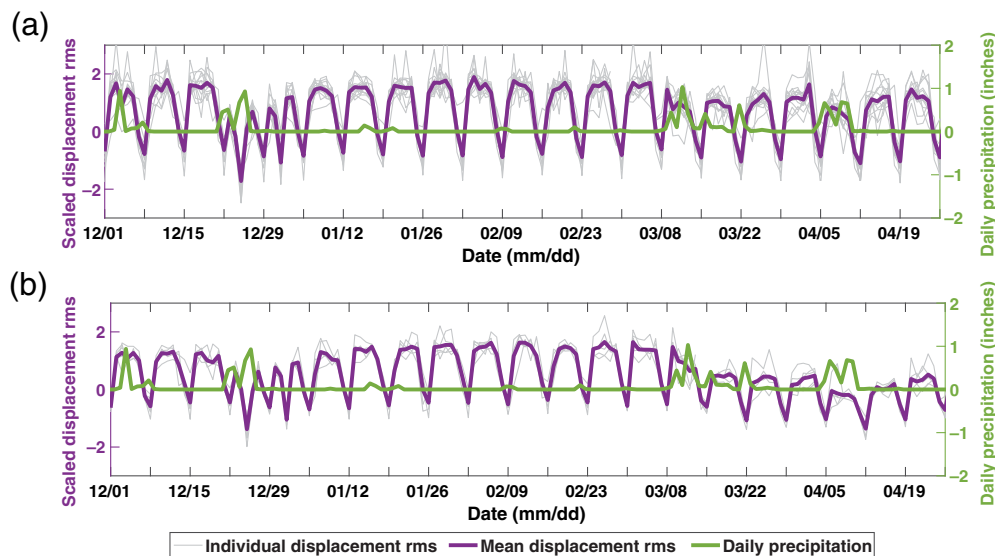


Figure 8. (a) Comparisons between the average daily precipitation in southern California and the 14 daily displacement rms time series that do not show a significant drop in amplitude after the “shelter-in-place” order. Gray thin curves are the individual time series of the 14 stations. Purple curves are the mean variation of the 14 individual time series. Green curves are the average daily precipitation time series over the 14 areas that are covered by the National Weather Service (NWS) office in Los Angeles–Oxnard and in San Diego. (b) Comparisons between the average daily precipitation in southern California and the five daily displacement rms time series that show a significant drop in amplitude after the shelter-in-place order. Gray thin curves are the individual time series of the five stations. Purple curves are the mean variation of the five individual time series. Green curves are the average daily precipitation time series in southern California (same as a). The color version of this figure is available only in the electronic edition.

(5–11 April). This drop correlates with a period of heavy precipitation in southern California (Fig. 8). This correlation could potentially be explained by traffic drop caused by an unfavorable weather condition. In the same period, the four stations that do not appear to be sensitive to human-activity variation show no drop in displacement rms amplitude (Fig. S4), meaning that the drop of displacement rms amplitude in Figure 8 during the week of 5–11 April probably is not due to a change in subsurface seismic structure induced by the increase of rainfall.

In summary, traffic activity appears to be able to explain all the observations we have so far; therefore, we consider the traffic activity to be the major noise source at 4–14 Hz for the 19 stations that show anthropogenic noise characteristics. This hypothesis can be further tested in a future study.

Why does the anthropogenic noise source not drop in many southern California stations?

Our results suggest that the behaviors of anthropogenic seismic noise after the shelter-in-place order are very diverse. If we assume that the level of anthropogenic seismic noise is, at least, somewhat proportional to the level of the human activity that causes it, our results above would imply that the seismic-noise-causing human activities responded differently to the shelter-

in-place order at different locations. Near the vicinity of some stations, these human activities drop during the shelter-in-place, as they did in the Christmas–New Year break; whereas, for others, these human activities did not drop. What is the reason behind this spatial variability?

It is nontrivial to fully address this question across the whole dataset. Here, we propose a hypothesis based on the comparison between CI.MSJ and CI.RSS, and on the authors’ experience in the Riverside area. As shown in Figure 9a, CI.MSJ is located on the Mt. San Jacinto College campus, and the CI.RSS station is located on the University of California, Riverside (UC Riverside) campus. Figure 9b plots the daily median displacement rms time series of these two stations. The top panel is CI.MSJ, and the bottom panel is CI.RSS. Blue curves show the trends of the

pandemic affected year (December 2019 to April 2020), and gray lines show the trends of the previous year in the same period (December 2018 to April 2019). In both the time series of CI.MSJ and CI.RSS, displacement rms dropped to a low level during the 2019 Christmas holiday and gradually climbed back to a high level in January 2020. As the COVID-19 situation intensified in early March 2020, Mt. San Jacinto College closed its campus on Friday, 13 March (Schultz, 2020). On 16 March, UC Riverside also closed its campus (Smith, 2020). Purple dashed lines denote the timing of when the two schools closed their campuses. Both of the campuses closed after the shelter-in-place order. However, the displacement rms time series only shows a significant drop in amplitude on the CI.MSJ record, not on the CI.RSS record.

As we discuss earlier, traffic activities would most likely be the noise sources at CI.MSJ and CI.RSS. If that is the case, why does the traffic activity drop near CI.MSJ, whereas, not in CI.RSS, even though they are only 40 km apart? We propose that it is because of the difference in traffic type. Immediately adjacent UC Riverside are California State Routes 60 and 91, and interstate Highway 215, all of which are designated as part of the Primary Freight Network System of the United States (link of the map provided in the Data and Resources), in which the Federal Highway Administration defines as “the most

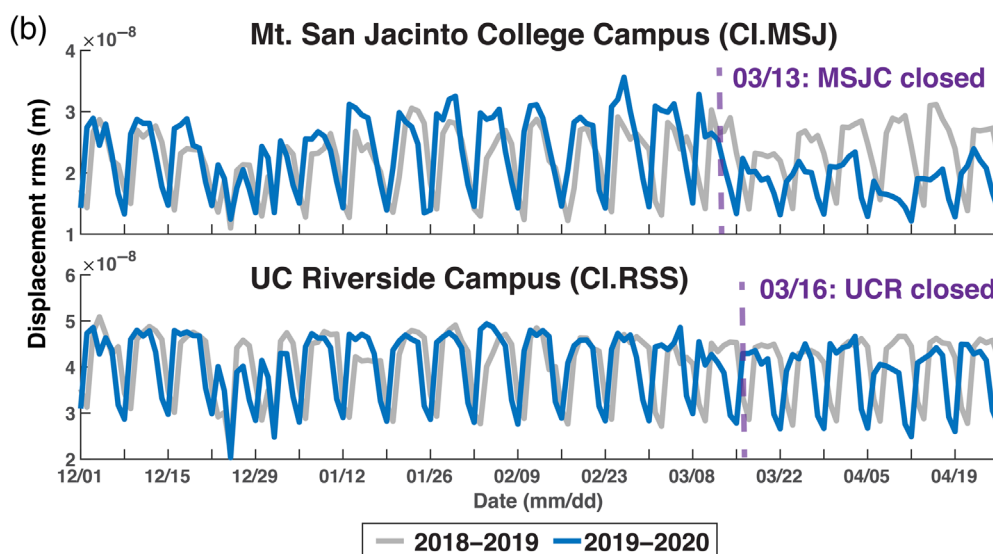
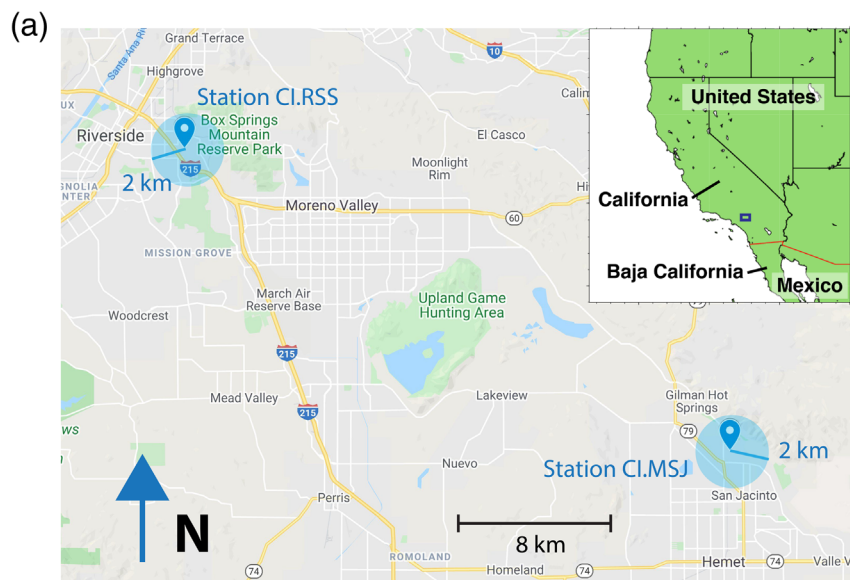


Figure 9. (a) Map showing the area near stations CI.MSJ and CI.RSS (Hemet area and Riverside area, California). The inset shows the map of California and its neighboring states. The blue rectangle in the inset map denotes the map extent of panel (a). Blue circular shading denotes an area within 2 km range of the station. The human-activity-induced seismic waves that are detected by the stations are mostly generated within the shaded area. (b) Daily median displacement rms time series of CI.MSJ (upper panel) and CI.RSS (lower panel) from 1 December to 26 April. In each panel, blue curves show the trends from December 2019 to April 2020, and gray curves show the trends from December 2018 to April 2019. The purple vertical dashed lines denote the dates when a “school close order” was implemented. The color version of this figure is available only in the electronic edition.

critical highway portions of the U.S. freight transportation system determined by measurable and objective national data.” The traffic related to such essential activities may not reduce after the shelter-in-place order. The nearest highway to Mt. San Jacinto College is located over 10 miles away, and, therefore, the noise at the station may be mainly related to local traffic, which may have been more strongly affected by the shelter-in-

place order. This hypothesis can be tested more comprehensively in a future study.

Comparing displacement rms time series with Apple mobility “driving index”

There are some independent datasets on human activity that are provided by smartphone-based mapping services. These smartphone-based mobility indices reflect the human activity in the larger metropolitan area, whereas, the displacement rms should reflect the human-activity level in the local area (within several kilometers). Therefore, it might be beneficial for us to compare these two similar but different types of dataset. Here, we compare our displacement rms time series with the Apple mobility “driving index.” The Apple mobility “driving index” is one of the mobility trends released by the Apple Inc., which are calculated based on the requests for directions in Apple Maps (details are in the [Data and Resources](#)). The data show a relative volume of direction requests per country, region, subregion, or city, compared to a baseline volume on 13 January 2020. Details about what city or subregion we select can be found in Text S4.

In Figure 6a, we compare our displacement rms trends in southern California, with the Apple mobility “driving index” of Los Angeles City (blue dashed curve). The Apple mobility “driving index” is similar to the displacement rms. It has a weekly periodic pattern that its amplitude is high on weekdays whereas low on weekends. Noticeably, the Apple mobility “driving index” always gradually increases during the weekdays and peaks on Fridays, which is different from the flat weekday-trend observed in displacement rms. A robust determination of this difference is out of the scope

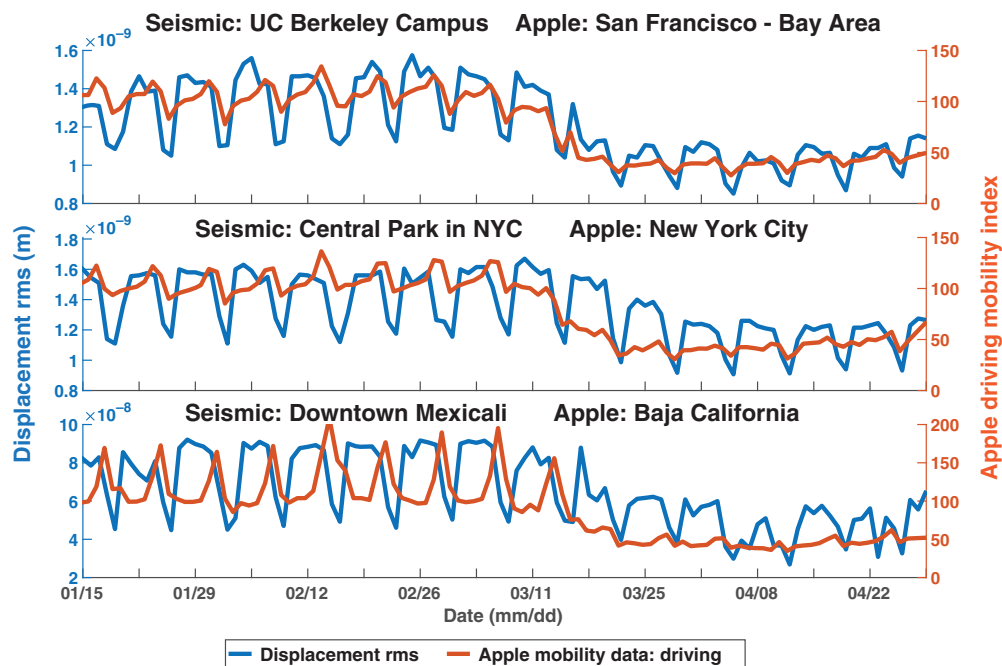


Figure 10. Comparisons between the ground vibration amplitude and the Apple mobility “driving index.” From top to bottom are BK.BRK, LD.CPNY, and BC.UABX stations, respectively. In each panel, blue curves show the trends of daily median displacement rms from December 2019 to April 2020, and orange curves show the Apple mobility “driving index” trends in the same period. The color version of this figure is available only in the electronic edition.

of this article. After the shelter-in-place order was implemented, the Apple mobility “driving index” dropped about 50%, implying that the average driving activity in the region was reduced in compliance with the order. However, as we discussed earlier, the displacement rms only drops in some stations, whereas, not in many others.

To further investigate the difference between seismic and smartphone-based data, we compare the displacement rms with the Apple mobility “driving index” for the three stations we investigate in the last [Result](#) section: BK.BRK, LD.CPNY, and BC.UABX (Fig. 10). As shown in the figure, the displacement rms drops recorded by seismometers are consistent with the decrease in Apple mobility “driving index,” in general. The differences in details may reflect the particular conditions in the local area near the seismometer. For example, the Apple mobility “driving index” in Baja California started to drop several days earlier than the displacement rms in downtown Mexicali. Similarly, the Apple mobility “driving index” in New York City shows a minimum in activity on around 20 March, whereas, the displacement rms at LD.CPNY near Central Park reached its lowest level, one week later on around 27 March.

The differences between the Apple Mobility Trend data and the displacement rms time series suggest that the independent measures of human activity are sensitive to different but complementary aspects of the pandemic response. The

displacement rms should reflect the human-activity level in the local area (within several kilometers), whereas, the Apple Mobility Trend should reflect human activity in the larger metropolitan area. By considering both the similarities and differences, it may help us to better characterize human behavior to the pandemic.

Conclusions

In this article, we use seismic data to extract information on human-activity changes during the early stage of the global COVID-19 pandemic in California, United States, New York City, United States, and Mexicali, Baja California, Mexico. We show that the displacement rms at 4–14 Hz has the ability to monitor human activity at a very local (several kilometers range) scale. Although, these data are to

first-order consistent with mitigation measures of the greater metropolitan area, the ground-motion data reveal unique information about the local area. In southern California, we observe that, although, some stations record a drop in human activity comparable to the Christmas holiday period, most stations do not. Considering the similarity in displacement rms time series between different stations and some evidence that indicate the noise back azimuth, we argue that traffic activities are very likely the noise source at 4–14 Hz for the 19 stations that show anthropogenic noise characteristics. Based on this argument, we propose that it is the difference in traffic type that determines whether the seismic noise drops near a station or not. For stations, such as CI.RSS, their nearby traffic activities include significant freight traffic. This traffic is likely related to essential activities and may not reduce after the shelter-in-place order. Conversely, for stations such as CI.MSJ, their nearby traffic activities are likely dominated by commuter traffic. Such traffic may be strongly affected by the shelter-in-place order, and the displacement rms would drop.

We investigate two other stations outside California, United States: station LD.CPNY in Central Park, New York City, United States, and station BC.UABX near downtown Mexicali, Baja California, Mexico. The drop in displacement rms of LD.CPNY near the Central Park area in New York City is delayed by, approximately, one week from the decrease

in human activity in New York City, determined by the Apple mobility “driving index.” Station BC.UABX records a drop in human activity during the COVID-19 pandemic. However, the timing of its drop is better correlated with the date of shelter-in-place order in its neighboring US state of California, rather than the date of implementation of shelter-in-place order in Mexico. These results suggest that the displacement rms is sensitive to much localized human-activity change and is thus capable of helping us better characterize the human behavior in response to COVID-19 pandemic.

Although, a seismometer is the best known for its ability to record earthquake shaking, it is also capable of recording ground movements caused by human activity, as we explore in this article. In particular, we have shown that the seismic noise at 4–14 Hz is, particularly, sensitive to the human-activity changes at a very local (several kilometers range) scale. The reduction in human activity during the pandemic offers us a chance to explore the nature of anthropogenic seismic noise in the seismic record, such as its physical origins and its attenuation with distance. In addition, the advancements of open-access seismic data make it possible for a daily monitoring of human activity via seismic noise in near-real-time, as opposed to a smartphone-based mobility index that could have a data lag of a couple of weeks. If interpreted properly, the seismic noise data can provide useful information on human activity that responds to the pandemic at a very local scale.

Data and Resources

All seismic data we used are open access at different data centers and can be accessed through the International Federation of Digital Seismograph Networks (FDSN) webservices (<https://www.fdsn.org/webservices>, last accessed July 2020). We downloaded all our data using the `obspy.clients.fdsn` module of the open-source Python toolbox ObsPy. The data of Southern California Seismic Network (CI) are downloaded from the Southern California Earthquake Data Center (SCEDC). The data of Berkeley Digital Seismograph Network (BK) are downloaded from the Northern California Earthquake Data Center (NCEDC). The data of Lamont–Doherty Cooperative Seismographic Network (LD) and the Centro de Investigación Científica y de Educación Superior de Ensenada’s (CICESE) Seismic Network (BC) are downloaded from the Incorporated Research Institutions for Seismology Data Management Center (IRIS-DMC). The data of Raspberry Shake (AM) are downloaded from the Raspberry Shake Project (RASPIshake). The Apple Mobility Trends data are downloaded from <https://www.apple.com/covid19/mobility> (last accessed May 2020). The precipitation data in Southern California are downloaded from the National Weather Service (NWS) office website (<https://w2.weather.gov/climate/xmacis.php?wfo=lox>, for Los Angeles/Oxnard office data, last accessed June 2020; <https://w2.weather.gov/climate/xmacis.php?wfo=sgx>, for San Diego Office data, last accessed June 2020). All maps in the article are made with Google Maps (<https://www.google.com/maps>, last accessed July 2020). The map of the Primary Freight Network System of the United States can be found on https://ops.fhwa.dot.gov/freight/infrastructure/ismt/state_maps/states/california.htm.

This article contains a supplemental materials document (a word document). It includes (1) Text S1, details of the method to compute displacement rms. (2) Text S2, details of the method to determine the direction of maximum horizontal amplitude. (3) Text S3, the method to calculate the seismic noise probability density function (PDF). (4) Text S4, details about how we select a city or subregion in the Apple Mobility Trends Reports. (5) Text S5, how we compute the average daily precipitation of southern California. (6) Text S6, a brief review of social-distancing measures in our study region that are potentially related to the timing of seismic noise drop. (7) Figure S1, the same figure as Figure 2c, except that the y axis is extended to include the maximum displacement rms of the 30 min long sliding window. (8) Figure S2, cross-correlation function between CI.RSS and CI.RVR. (9) Figure S3, instrument response functions. (10) Figure S4, the displacement rms time series of the four stations that are not capable of reflecting human-activity variation.

Declaration of Competing Interests

The authors acknowledge that there are no conflicts of interest recorded.

Acknowledgments

The authors are grateful to Daniel McNamara and Stephen Hicks for constructive reviews that greatly improved the article. The authors thank Thomas Lecocq for sharing the SeismoRMS code package and making a very easy-to-understand Jupyter Notebook tutorial for everyone. This research was initiated and developed in the seismology journal club at the Earth and Planetary Sciences Department at University of California, Riverside. The authors want to thank all the participants (and their families and friends!) for discussing the results and providing input with their life experience in the study area. This work was supported by the College of Natural and Agricultural Sciences (CNAS) at University of California, Riverside, as part of its Core Membership in the Southern California Earthquake Center (SCEC). Baoning Wu was, in part, supported by the University of California President’s Dissertation-Year Fellowship.

References

- Arango, T., and J. Cowan (2020). Gov. Gavin Newsom of California orders Californians to stay at home [online], *The New York Times*, 19 March 2020, available at <https://www.nytimes.com/2020/03/19/us/california-stay-at-home-order-virus.html> (last accessed July 2020).
- Bensen, G. D., M. H. Ritzwoller, M. P. Barmin, A. L. Levshin, F. Lin, M. P. Moschetti, N. M. Shapiro, and Y. Yang (2007). Processing seismic ambient noise data to obtain reliable broad-band surface wave dispersion measurements, *Geophys. J. Int.* **169**, no. 3, 1239–1260.
- Berkeley News (2020). As coronavirus spreads, UC Berkeley suspends in-person instruction [online], University of California, *Berkeley website*, 9 March 2020, available at <https://news.berkeley.edu/2020/03/09/as-coronavirus-spreads-uc-berkeley-suspends-in-person-instruction/> (last accessed July 2020).
- Bonaccorsi, G., F. Pierri, M. Cinelli, A. Flori, A. Galeazzi, F. Porcelli, A. L. Schmidt, C. M. Valensise, A. Scala, W. Quattrocioni, *et al.* (2020). Economic and social consequences of human mobility restrictions under COVID-19, *Proc. Natl. Acad. Sci.* **117**, no. 27, 15,530–15,535.

- California Institute of Technology and U.S. Geological Survey Pasadena (1926). Southern California seismic network, International Federation of Digital Seismograph Networks, doi: [10.7914/SN/CI](https://doi.org/10.7914/SN/CI).
- California Office of the Governor (2020). Governor Newsom declares state of emergency to help State prepare for broader spread of COVID-19 (press release) [online], 4 March 2020, available at <https://www.gov.ca.gov/2020/03/04/governor-newsom-declares-state-of-emergency-to-help-state-prepare-for-broader-spread-of-covid-19/> (last accessed July 2020).
- Casiano, L. (2020). California Gov. Gavin Newsom announces statewide coronavirus 'stay at home' order [online], *Fox News*, 19 March 2020, available at https://www.foxnews.com/us/california-gov-gavin-newsom-announces-statewide-stay-at-home-order.amp?cmpid=prn_newsstand (last accessed July 2020).
- Fry, W. (2020). Baja California to use police and military forces to keep people inside [online], *The San Diego Union-Tribune*, 30 March 2020, available at <https://www.sandiegouniontribune.com/news/border-baja-california/story/2020-03-30/baja-california-to-deploy-military-forces-to-keep-people-inside> (last accessed July 2020).
- Gibney, E. (2020). Coronavirus lockdowns have changed the way Earth moves, *Nature* **580**, no. 7802, 176.
- Guenaga, D. L., O. E. Marcillo, A. A. Velasco, C. Chai, and M. Maceira (2021). The silencing of U.S. campuses following the COVID-19 response: Evaluating root mean square seismic amplitudes using power spectral density data, *Seismol. Res. Lett.* **92**, 941–950, doi: [10.1785/0220200391](https://doi.org/10.1785/0220200391).
- Havskov, J., and G. Alguacil (2016). *Instrumentation in Earthquake Seismology*, Chapter 3, Springer, Switzerland, 101–111, doi: [10.1007/978-3-319-21314-9](https://doi.org/10.1007/978-3-319-21314-9).
- Kraemer, M. U., C. H. Yang, B. Gutierrez, C. H. Wu, B. Klein, D. M. Pigott, L. Du Plessis, N. R. Faria, R. Li, W. P. Hanage, et al. (2020). The effect of human mobility and control measures on the COVID-19 epidemic in China, *Science* **368**, no. 6490, 493–497.
- Lecocq, T., S. P. Hicks, K. Van Noten, K. Van Wijk, P. Koelemeijer, R. S. M. De Plaen, F. Massin, G. Hillers, R. E. Anthony, M. T. Apoloner, et al. (2020). Global quieting of high-frequency seismic noise due to COVID-19 pandemic lockdown measures, *Science* doi: [10.1126/science.abd2438](https://doi.org/10.1126/science.abd2438).
- Lewis, B. (2020). Baja California battling coronavirus, residents urged to stay home [online], *CBS 8*, 1 April 2020, available at <https://www.cbs8.com/article/news/health/coronavirus/baja-california-battling-coronavirus-residents-urged-to-stay-home/509-26f77b1e-ae07-4aee-afc8-392ae74a3d10> (last accessed July 2020).
- Linder, M. (2020). California's first case of coronavirus confirmed in Orange County [online], *NBC Bay Area*, 26 January 2020, available at <https://www.nbcbayarea.com/news/california/first-case-of-coronavirus-confirmed-in-californias-orange-county/2221025/> (last accessed July 2020).
- Matrajt, L., and T. Leung (2020). Evaluating the effectiveness of social distancing interventions to delay or flatten the epidemic curve of coronavirus disease, *Emerg. Infect. Dis.* **26**, no. 8, 1740.
- McNamara, D. E., and R. P. Buland (2004). Ambient noise levels in the continental United States, *Bull. Seismol. Soc. Am.* **94**, no. 4, 1517–1527.
- New York Office of the Governor (2020). Governor Cuomo signs the 'New York State on PAUSE' executive order (Press release) [online], 20 March 2020, available at <https://www.governor.ny.gov/news/governor-cuomo-signs-new-york-state-pause-executive-order> (last accessed July 2020).
- Peterson, J. R. (1993). Observations and modeling of seismic background noise, *U.S. Geol. Surv. Open-File Rept.* 93-322, doi: [10.3133/ofr93322](https://doi.org/10.3133/ofr93322).
- Poli, P., J. Boaga, I. Molinari, V. Cascone, and L. Boschi (2020). The 2020 coronavirus lockdown and seismic monitoring of anthropic activities in Northern Italy, *Sci. Rep.* **10**, no. 1, 9404, doi: [10.1038/s41598-020-66368-0](https://doi.org/10.1038/s41598-020-66368-0).
- Public Health Department, County of Santa Clara (2020). Seven Bay area jurisdictions order residents to stay home (Press release) [online], 16 March 2020, available at <https://www.sccgov.org/sites/phd/news/Pages/press-release-03-16-20.aspx> (last accessed July 2020).
- Schultz, R. (2020). MSJC closing all locations until 4/6 (school announcement) [online], Mt. San Jacinto College website, 13 March 2020, available at <https://www.msjc.edu/coronavirus/message-to-students-2020-03-13.html> (last accessed July 2020).
- Smith, T. (2020). UCR campus "closed" (school announcement) [online], University of California, Riverside, California 14 March 2020, available at <https://insideucr.ucr.edu/announcements/2020/03/14/ucr-campus-closed> (last accessed July 2020).
- Stutzmann, E., G. Roullet, and L. Astiz (2000). GEOSCOPE station noise levels, *Bull. Seismol. Soc. Am.* **90**, no. 3, 690–701.
- Tanimoto, T., S. Ishimaru, and C. Alvizuri (2006). Seasonality in particle motion of microseisms, *Geophys. J. Int.* **166**, no. 1, 253–266.
- Thunström, L., S. C. Newbold, D. Finnoff, M. Ashworth, and J. F. Shogren (2020). The benefits and costs of using social distancing to flatten the curve for COVID-19, *J. Benefit-Cost Anal.* 1–27.
- Wick, J. (2020). Newsletter: Newsom to 40 million Californians: Stay home [online], *Los Angeles Times*, 20 March 2020, available at <https://www.latimes.com/california/newsletter/2020-03-20/california-stay-home-newsom-coronavirus-newsletter-essential-california> (last accessed July 2020).
- Wigglesworth, A., R. Lin II, and S. Kohli (2020). California's first two cases of coronavirus are confirmed in L.A. and Orange counties [online], *Los Angeles Times*, 26 January 2020, available at <https://www.latimes.com/california/story/2020-01-25/los-angeles-area-prepared-for-coronavirus> (last accessed July 2020).
- Xiao, H., Z. Eilon, C. Ji, and T. Tanimoto (2020). COVID-19 societal response captured by seismic noise in China and Italy, *Seismol. Res. Lett.* **91**, no. 5, 2757–2768.

Manuscript received 27 July 2020

Published online 07 April 2021